Proc. *4th Int. Conf. Remote Sensing for Marine and Coastal Environments*, ERIM, Ann Arbor, vol. 2, 13-22.

OPTICAL PROPERTIES OF SEDIMENT-LOADING MARINE WATERS : FIRST RESULTS ON THE INFLUENCE OF GOETHITE[1]

S. Ouillon*, P. Forget*, F. Lahet*, Y. Lucas**
* LSEET - ** LEPI
Université de Toulon et du Var
83957 La Garde, France

ABSTRACT

This paper presents experimental measurements of the attenuation coefficient spectrum of marine water loaded with two mineral components, goethite and kaolinite. Three different concentrations are considered. The measurements are done using a 1024-channel spectroradiometer in the range 400-900 nm. The experimental spectra after removal of pure seawater attenuation spectrum clearly exhibit a segment whose mean level linearly increases and whose slope in the blue-red interval linearly decreases with increasing concentration. The influences of the goethite refractive index, size distribution and sediment concentration on the mean spectral level and slope values are discussed using Mie scattering theory.

1.0 INTRODUCTION

The sea surface reflectance depends on the different constituents of the marine water. Empirical relationships are currently established between reflectance and total suspended matter concentration in order to calibrate satellite image data over specific sites (e.g. Forget and Ouillon, 1997). A more refined method takes into account the three major components of turbid coastal waters : phytoplankton, yellow substances and suspended sediments (Sathyendranath et al., 1989). Due to the few number of channels in present satellite-borne visible sensors, and due to the large bandwidth of the channels, these methods can give only a coarse description of the suspended matter. This limitation will be overcome by the performances of future multispectral sensors specifically dedicated to ocean color monitoring (e.g. SeaWiFS). But studies still need to be carried out for inverting these satellite data in terms of geophysical parameters and, especially, of parameters specifying the sediment constituents of coastal waters.

In the river outflows, the minerals having the most significant influence on the optical water properties are the iron oxides (goethite, hemathite, maghemite, lepidocrocite,...) which are strongly coloured. Transparent minerals, such as quartz or gibbsite, have only a slight influence on the water optical properties. This paper presents experimental measurements of the beam attenuation coefficient spectra of pure marine water and of marine water loaded with various concentrations of two major mineral components, goethite and kaolinite (white). The spectra are analyzed and discussed

---

1 Presented at the Fourth Thematic Conference on Remote Sensing for Marine and Coastal Environments, Orlando, Florida, 17-19 March 1997.

using Mie scattering theory (e.g. van de Hulst, 1957), which has been proved to be a valuable tool to study the attenuation and scattering properties of the marine water components (Stramski and Kieffer, 1991) and, thus, for remote sensing purposes, to study the sea reflectance which is closely related to these properties (Morel and Prieur, 1977; Kirk, 1993; Mobley, 1994).

2.0 METHODS

The beam attenuation $c(\lambda)$ of light in a medium is described by :

$$d\phi = - c(\lambda) \phi(z) dz \quad (1)$$

where ϕ is the radiant flux of a collimated light, $c(\lambda) = a(\lambda) + b(\lambda)$, $a(\lambda)$ and $b(\lambda)$ being the absorption and scattering coefficients of the medium, respectively, and dz the light path length.

2.1 EXPERIMENTAL METHODS

The beam attenuation is measured through a quartz cuvette of optical length 1 cm. The cuvette is illuminated by a Tungstene-Halogene light source, and measurements are done using a 1024-channel spectroradiometer (Ocean Optics) in the range 400-900 nm.

The turbid water samples are prepared by adding to clear marine water (total suspended matter less than 1 mg/l) amounts of a mineral with known properties. The beam attenuation coefficient spectrum of the clear marine water is shown on Figure 1. The beam attenuation coefficient spectrum proposed by Smith and Baker (1981) for the clearest natural waters is also reproduced.

Goethite is one of the major iron oxides contained in the river outflows. The mineral sample we used, BTS4, essentially consists of small, mainly spherical, goethite particles and of large kaolinite particles. On BTS4, goethite is composed of 70% by FeOOH and of 30 % by AlOOH. The detailed sample composition is reported on Table 1.

Table 1. Composition of the mineral sample used (BTS4).

Mineral		Amount
Kaolinite	$Si_2O_5Al_2(OH)_4$	79 %
Quartz	SiO_2	5 %
Gibbsite	$Al(OH)_3$	9 %
Goethite	α-FeO(OH)	2 %
Anatase	TiO_2	3 %
Heavy minerals		< 2 %

2.2 MIE THEORY

Mie theory allows to determine how the incident light at wavelength λ is absorbed and scattered by a sphere of diameter D and of refractive index $m_s = n_s - ik_s$, imbedded in a non-absorbing medium of index $m_m = n_m$. The scattering efficiency Q_b is the fraction of radiant energy incident on the sphere that is scattered into all directions. Likewise, other efficiencies can be defined : Q_a for absorption, $Q_c = Q_a + Q_b$ for total attenuation (extinction efficiency). These efficiencies depend on :

- the relative complex index of refraction m_r defined by

$$m_r = \left(\frac{n_s}{n_m}\right) - i\left(\frac{k_s}{n_m}\right) = n_r - ik_r \tag{2}$$

- the Mie size parameter α defined by :

$$\alpha = \frac{\pi D}{\lambda} \tag{3}$$

The absorption, scattering and beam attenuation coefficients $a(\lambda)$, $b(\lambda)$ and $c(\lambda)$, which are the bulk parameters as measured by optical instruments and as used in radiative transfer theory, are given by :

$$b(\lambda) = \int_{m_r}\int_{D} Q_b(D, m_r, \lambda) \quad \frac{\pi D^2}{4} \quad n(D) \quad dD \quad dm_r \tag{4}$$

$$c(\lambda) = \int_{m_r}\int_{D} Q_c(D, m_r, \lambda) \quad \frac{\pi D^2}{4} \quad n(D) \quad dD \quad dm_r \tag{5}$$

$$a(\lambda) = c(\lambda) - b(\lambda) \tag{6}$$

where $n(D)\ dD$ is the number of particles having a diameter in the range $[D,\ D+dD]$.

Mie theory necessitates to know important characteristics of the particles and, principally, their size distribution and their spectral refractive index.

3.0 EXPERIMENTAL RESULTS AND ANALYSIS

The optical measurements are performed on water samples with three different BTS4 concentrations : 120 mg/l, 220 mg/l and 390 mg/l. The relative uncertainty on Suspended Sediment

Concentration (SSC) measurements is 14%, 8% and 4.5 %, respectively. The experimental attenuation spectra, $c_e(\lambda)$, are presented on Figure 2. They result from an average of 10 up to 12 measurements for each concentration. It should be noted that the data at wavelengths less than 480 nm are noisy. This is due to the weakness of the signal emitted by the light source in that range, involving a great sensitivity in $d\phi/\phi$ determination (see Eq. 1).

In order to get the specific attenuation of the sediment, and owing to the classical additivity property of attenuation, the pure seawater attenuation spectrum of Figure 1 was substracted from the experimental spectra. The resulting spectra, $c_f(\lambda)$, are shown on Figure 2. At high sediment concentrations, the rough $c_e(\lambda)$ spectra have three local minima in the vicinity of 410 nm, 710 nm and 815 nm, respectively. At low concentration, discontinuities are observed at these wavelengths and it may be concluded by comparing $c_e(\lambda)$ and $c_f(\lambda)$ spectra that sea water attenuation properties are responsible for these features.

At each wavelength, we find a linear variation of spectral values with concentration, as illustrated on c_f(600 nm) on Figure 3. Inspection of $c_f(\lambda)$ spectra shows an interesting feature consisting in a quasi-linear variation with wavelength from 450 nm with a slope decreasing when concentration increases. The slope values of c_e and c_f spectra, called s_e and s_f respectively, are listed in Table 2 and sketched versus SSC on Figure 4.

Table 2. Beam attenuation coefficient at 500, 600 and 700 nm, and slopes of the spectra in the range 500-700 nm, for Suspended Sediment Concentrations (SSC) of 1, 120, 220 and 390 mg/l.

	SSC = 1 mg/l	SSC = 120 mg/l	SSC = 220 mg/l	SSC = 390 mg/l
c_{500} (m^{-1})	0.310	16.597	36.543	69.19
c_{600} (m^{-1})	0.704	16.602	35.755	66.74
c_{700} (m^{-1})	1.108	16.667	35.195	64.72
$s_{e\ 500\text{-}700}$ ($m^{-1}.\mu m^{-1}$)	3.99	0.35	- 6.74	- 22.36
$s_{f\ 500\text{-}700}$ ($m^{-1}.\mu m^{-1}$)	0.0	- 3.64	- 10.73	- 26.35

4.0 DISCUSSION USING MIE THEORY

Mie theory is used to retrieve the attenuation coefficient from the particle characteristics and concentrations. We consider the spectral refractive index given by Bedidi and Cervelle (1993) relative to goethite. Several types of particle size distributions are considered.

The first computation is done with a same diameter for each mineral particle. A diameter of 7.5 µm allows to retrieve the mean experimental levels of attenuation for the three concentrations. The calculated attenuation spectrum is reported on Figure 5. We obtain straight lines with slightly positive slopes increasing with concentration.

In order to improve the results, we examine the effect of a natural size distribution. The Junge (also called hyperbolic) size distribution describes many natural families of particles such as fine suspended particles in sea water (Bader, 1970), following :

$$n(D) = k \quad D^{-r} \quad (m^{-3}) \tag{7}$$

where k sets the scale by taking into account the nature, size and concentration of the particles. A value of r=4 approximates well both mineral and chlorophyll distributions (Nanu and Robertson, 1993). Choosing a particle size from 7 to 10 µm, we also obtain straight lines with positive slopes increasing when concentration increases, but their mean values are lower (see Figure 6). The agreement between experimental and theoretical levels is less satisfactory.

In the previous calculations, we imposed the refractive index of goethite to all the minerals of the sample, considering that each of them was optically active. In fact, the sample is composed of small goethite particles (D < 1µm) and of larger kaolinite particles. These latter, due to their diameter, have a weak optical influence. Another way consists in isolating the effect of goethite, whose amount was determined by a laser analyzer. The particle size distribution shows a peak at about 0.3 µm, which corresponds to 2% of the total volume. Assuming that this feature is only due to goethite, the new input parameters of the model are D = 0.26 µm and a concentration equal to 0.02 *SSC*. The results are reported on Figure 7. The attenuation values computed at each wavelength, with a varying spectral refractive index, are scattered, but the straight line obtained by linear regression has now a negative slope, whose absolute value increases with increasing concentration. The scatter of the data can be explained by the high sensitivity of the model to refractive index m_r for D in the range 0.1-0.3 µm.

In order to explain the observed negative slope of the attenuation coefficient, we compute the attenuation efficiency Q_c versus particle diameter D at two wavelengths, 500 and 700 nm. The results are reported on Figure 8. We observe that Q_c is constant for D > 1 µm, and that Q_c is greater at 500 µm than at 700 µm for particles having a diameter less than 0.28 µm. This explains the results reported on Figures 5 and 6, and that the negative slope obtained from measurements can not be due to large particles.

5.0 CONCLUSION

Experimental measurements of the attenuation coefficient spectrum of marine water loaded with two mineral components, goethite and kaolinite, for three different concentrations, were presented. The experimental spectra after removal of pure seawater attenuation spectrum clearly exhibit a linear segment whose mean level linearly increases and whose slope in the blue-red interval linearly decreases with increasing concentration. Computations made using Mie scattering

theory indicate that the smallest particles (goethite) are responsible for the slope of the spectra, whereas the mean level depends on their concentration. In order to improve the study, future computations are to be made taking into account both the particle size distribution and the spectral refractive index relative to each particle size.

6.0 ACKNOWLEDGEMENTS

This study was supported by the European Community Environment Research Program MAST 3, contract FANS MAS3-CT95-0037.

7.0 REFERENCES

H. Bader, The hyperbolic distribution of particle sizes, *J. Geoph. Res.*, 75, n°15, 2822, 1970.

A. Bedidi and B. Cervelle, Light scaterring by spherical particles with hemathite ang goethi-telike optical properties : effect of water impregnation, *J. Geoph. Res.*, 98, n°B7, 11941-11952, 1993.

P. Forget and S. Ouillon, Surface suspended matter off the Rhône river mouth from visible satellite imagery, submitted to *Oceanologica Acta*, 1997.

J.T.O. Kirk, *Light and Photosynthesis in Aquatic Ecosystems*, Cambridge Univ. Press, 401 pp, 1995.

C. Mobley, *Light and Water*, Academic Press, 592 pp, 1994.

A. Morel and L. Prieur, Analysis of variations in ocean color, *Limn. Ocean.*, 22, 709-722, 1977.

L. Nanu and C. Robertson, The effect of suspended sediment depth distribution on coastal water spectral reflectance : theoretical simulation, *Int. J. Remote Sensing*, 14, n°2, 225-239, 1993.

S. Sathyendranath, A. Morel and L. Prieur, A three-component model of ocean colour and its application to remote sensing of phytoplancton pigments in coastal waters, *Int. J. Remote Sensing*, 10, n°8, 1373-1394, 1989.

R.C. Smith and K. Baker, Optical properties of the clearest natural waters, *Appl. Opt.*, 20, n°2, 177-184, 1981.

D. Stramski and D.A. Kiefer, Light scattering by microorganisms in the open ocean, *Prog. Oceanog.*, 28, 343-383, 1991.

H.C. van de Hulst, *Light scattering by small particles*, John Wiley & Sons, Inc., New York, 1957.

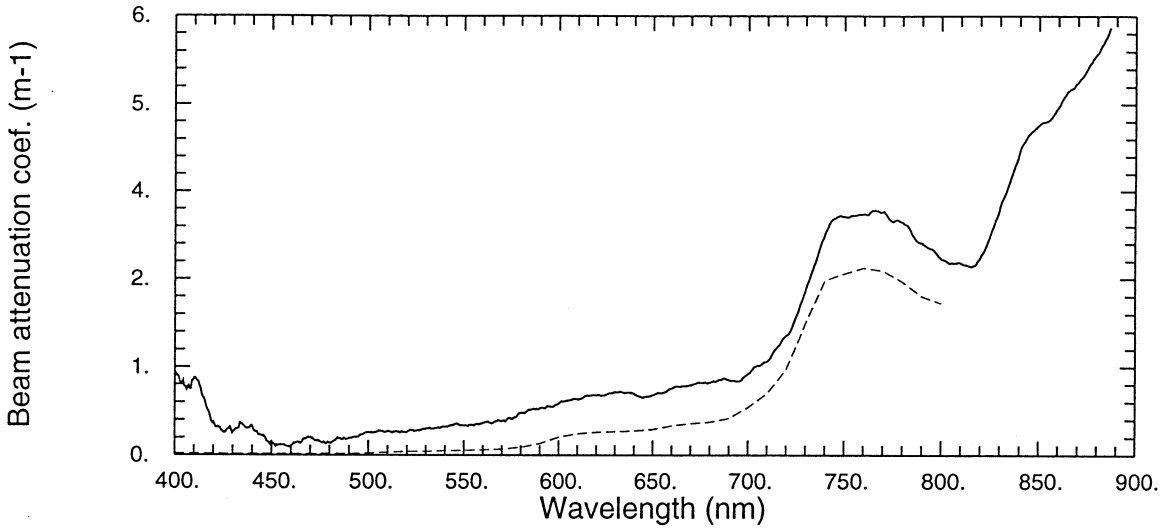

Figure 1. Beam attenuation spectrum of clear marine water.
____ marine water used in this study
- - - clearest natural waters (Smith and Baker, 1981)

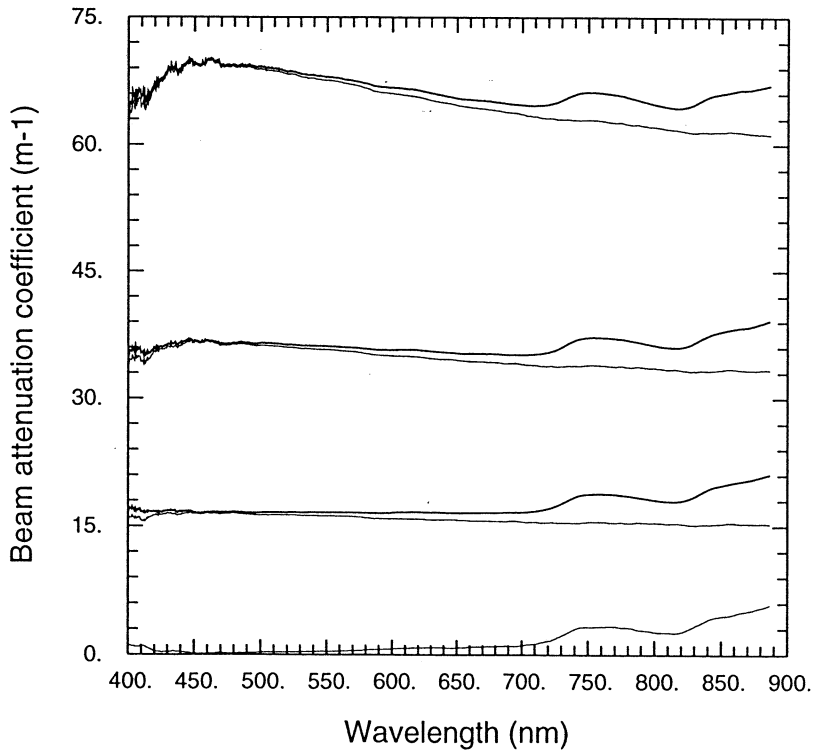

Figure 2. Beam attenuation coefficient spectra.
A: SSC = 1 mg/l ; B: SSC = 120 mg/l ; C: SSC = 220 mg/l ; D: SSC = 390 mg/l
total beam attenuation coefficient (water+minerals) : c_e (bold)
total beam attenuation - beam attenuation of used marine water : c_f (fine)

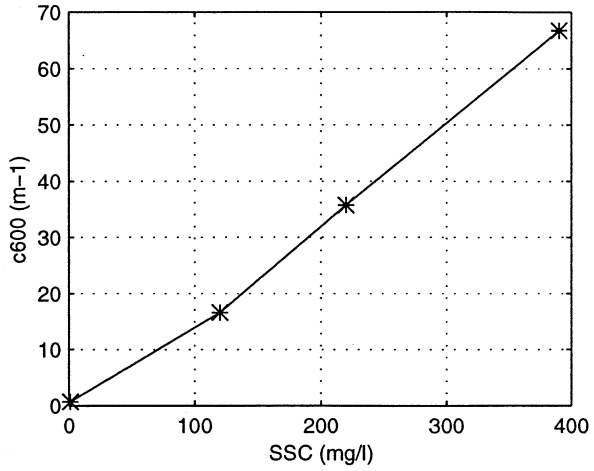

Figure 3. Measured beam attenuation coefficient versus SSC at 600 nm.

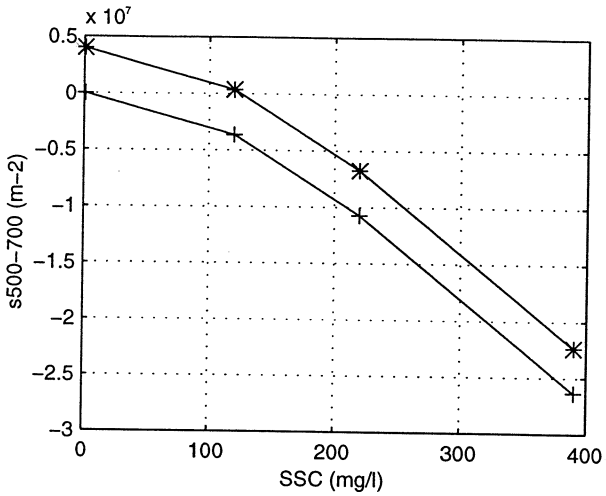

Figure 4. Slope of the beam attenuation coefficient spectrum versus SSC and versus wavelength. * s_e + s_f

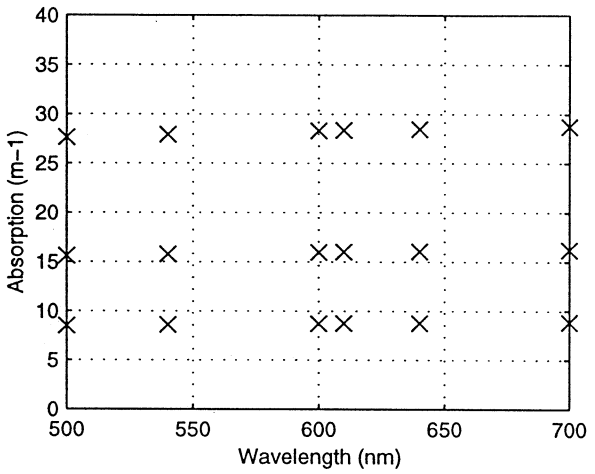

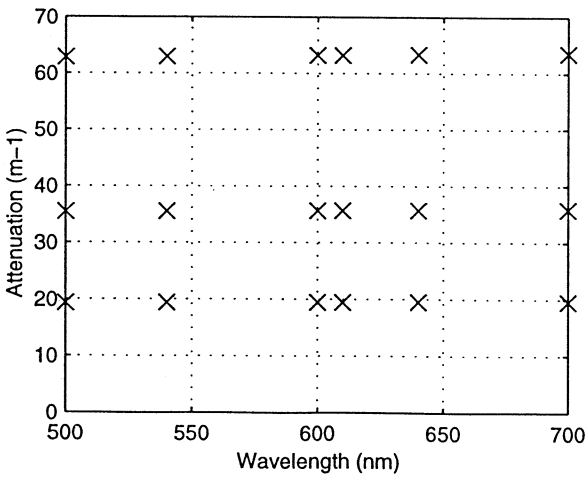

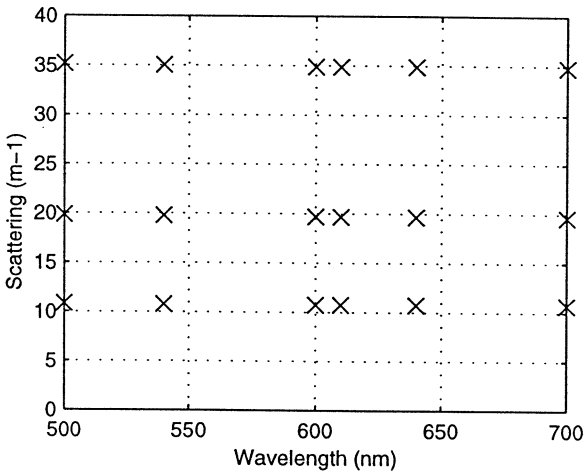

Figure 5. Calculated beam absorption, scattering and attenuation coefficients versus SSC. D = 7.5 μm

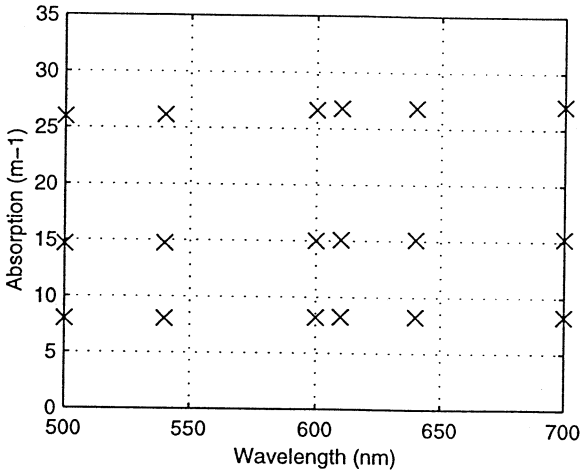

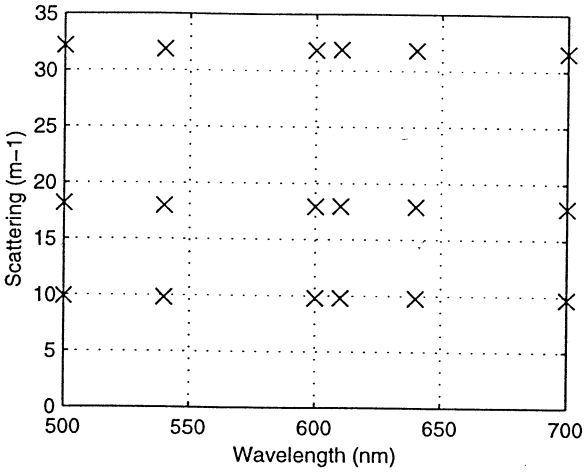

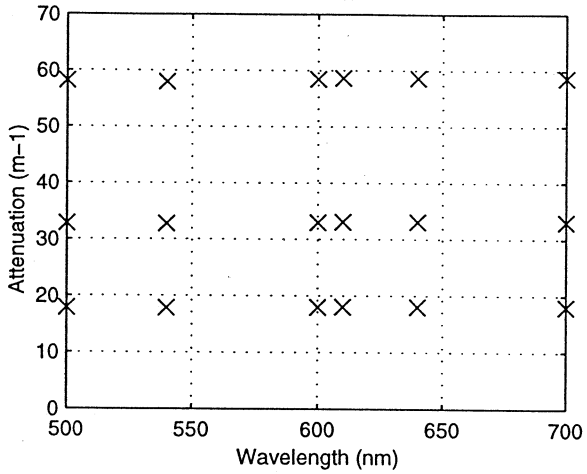

Figure 6. Calculated beam absorption, scattering and attenuation coefficients versus SSC. 7 μm < D < 10 μm

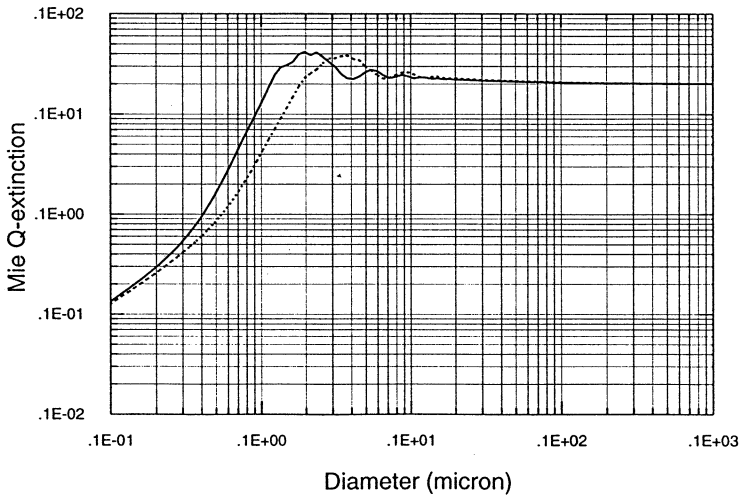

Figure 8. Attenuation efficiency of a goethite particle versus its diameter D. ___ 500 nm, --- 700 nm

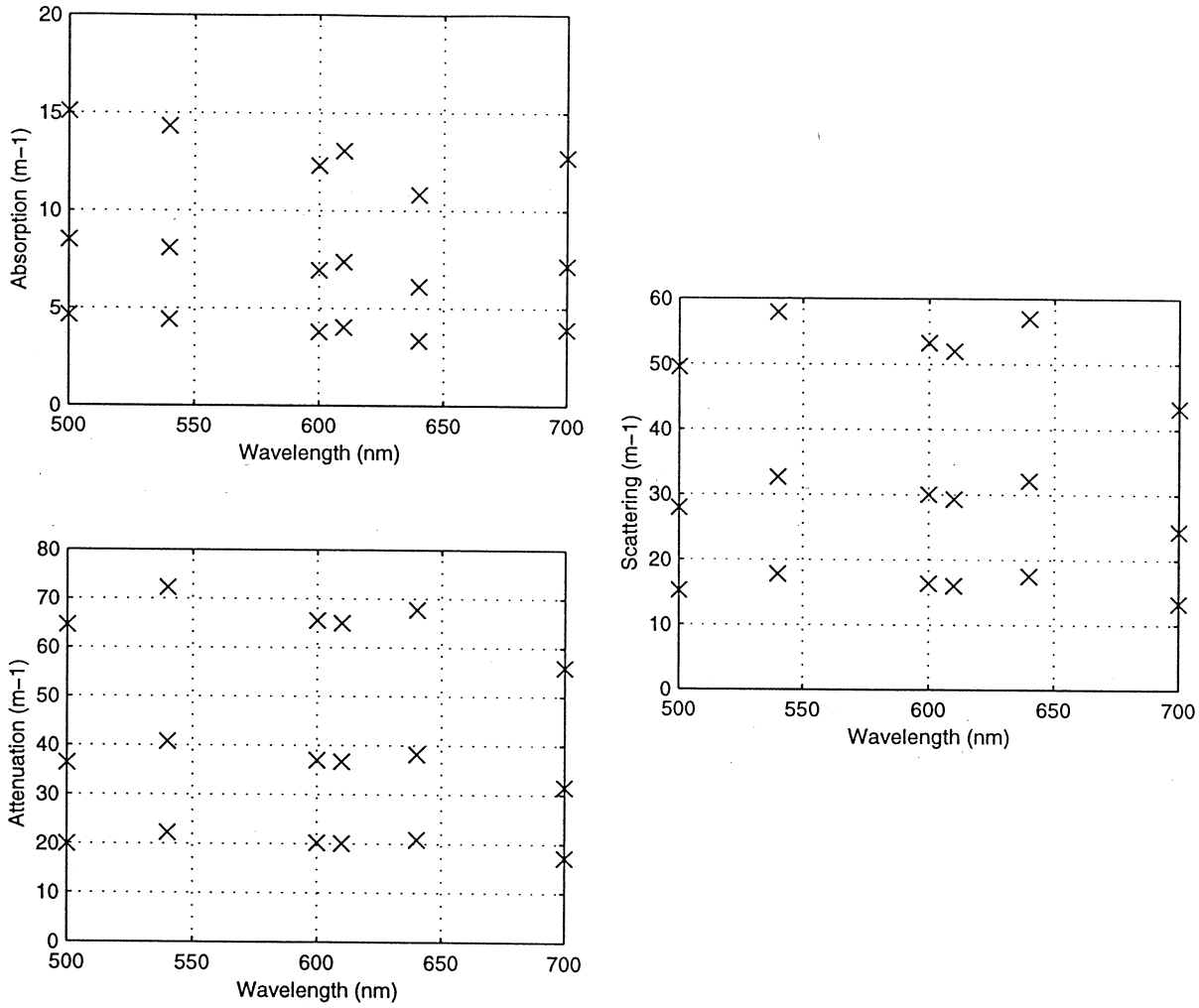

Figure 7. Calculated beam absorption, scattering and attenuation coefficients versus SSC. D = 0.26 μm, $C_{goethite}$ = 0.02 SSC